

Responses to reviewer comments for the article “Using observations of surface fracture to address ill-posed ice softness estimation over Pine Island Glacier”

We would like to thank the editor and reviewers very much for the taking the time to read the article and for providing us with valuable and insightful feedback. All reviewer comments and responses are collated in this document. Each review is reproduced here in full. Responses to any general comments of the reviewers are coloured in teal, while responses to specific comments are tabulated afterwards.

A central theme of both reviews is that parts of the article should be restructured to make it easier to follow. To this end, I have made various structural changes, informed by specific comments made by the reviewers, for example, moving text between the introduction and methods sections. We hope the reviewers find that these changes have improved the flow and clarity of the article.

Responses to comments from Reviewer #1

Reviewer 1: In this manuscript, the authors investigate the effect of assimilating more prior information into inversions for ice stiffness. The data informing the priors are strain rates, and locations of fracture derived from satellite imagery. Pine Island is chosen as a study area due to the large amount of fracturing observed there. Experiments are carried out using both snapshot and time-dependent inversion processes, using different regularisation. The results show that the use of this data in priors results in stiffness fields which better visually represent observed fracture patterns, without affecting the velocity misfit. The use of methods informed by fracture data could be important for improving inversions of floating ice, but is likely not have much impact on grounded areas. It is suggested that these methods would be best suited to diagnostic modelling and attempts to evolve stiffness fields through time.

This study will be valuable to a particular niche of ice flow modellers, and is certainly within the scope of The Cryosphere. I personally found it to be interesting, although I think wider interest will be limited as the focus is only on the inversion process and, by the authors' own admission, unlikely to be of much help to long-term predictive simulations.

My main issue with this manuscript is that it can be quite difficult to read, and is unclear at times. The introduction seems a little muddled, with some parts referencing specifics of this study among a more general review of the relevant issues. I would recommend moving anything specific to this study (sliding law, value of n in flow law etc.), and the more detailed discussion of reasoning behind the methods used found in the last paragraphs, into the methods section, so that it can all easily be found and doesn't over-complicate the introduction.

I also found the methods section difficult to follow in places. Section 2.1 would in my opinion benefit from being restructured. I also think the methods section should contain a clear summary of all the experiments which were carried out, as these are not all introduced until during the results section.

The scientific content of this manuscript is good, and worthy of publication, but I think work needs to be done to improve the clarity of its presentation. For this reason, I recommend publication after revisions.

Response: We would like to thank the reviewer for their positive comments about the article and their thorough and thoughtful review. I have restructured the introduction and methods sections (and the results to some degree) to make things clearer. Many of the changes made are in response to specific comments laid out in the review below.

Responses to specific comments from Reviewer #1

Reviewer 1		
ID	Reviewer Comment	Response
1	Line 27: Is this a typo, or is the approximately equal sign there for a reason? If not a typo, please explain what is meant and be clear what value for n is being used in your work.	This is not a typo, though I have made this less ambiguous by adding the sentence: “The value of the exponent n is dependent on the particular mechanisms by which creep occurs within the ice and various properties of the crystal grains (e.g. Haefeli (1961)), and takes a value between 1 and 4 in most cases. Here, we take the common reference value of $n = 3$ ”.
2	Line 30: It may be helpful to write Eq.1 in a form which includes $\phi(x)$ for clarity.	I have changed this sentence to be: Here, we consider the approach in which these are prescribed <i>a priori</i> and a ‘stiffness’ field $\phi(x)$ is defined over the domain to account for unknown deviations in the expected ice rheology, such that eq. 1 becomes $\tau_{ij} = 2\phi\eta\dot{\epsilon}_{ij}$
3	Line 43: I think the sliding law used in this study should be stated in the methods section rather than the introduction	Thank you, I have moved this line into the methods.
4	Lines 48-51: It’s a little unclear at points in this introduction whether you are talking about the specific process(es) used in your study, or more generally. As a more general point, some inversion processes use u and v velocity components as two separate observed fields, and some can also make use of thickness changes dh/dt . This doesn’t mean the problem is ever not ill-posed, but there is a greater variety in approaches that just using a single u field. If this statement is referring to the specific process used in this study, please make this clear.	I hope that the changes made to the introduction and methods have addressed the issue of clarity and distinguished statements that relate to methods in general and those we use ourselves in the article. I have also added a couple of sentences that make it clear that other data can be included in the inverse problem as suggested.
5	Lines 92-5: This detail probably belongs in the methods section	This has been moved into the methods.
6	Lines 97-102: As above, better to put the detail in methods.	This has also been moved into the methods

7	<p>Lines 113-4: Could this point about the link between dynamics and fracturing over the rest of Antarctica be expanded on in the discussion?</p>	<p>I appreciate the desire to expand on this, but I think it might be difficult to do so without moving into speculation. PIG has shown a strong connection between fracturing and broader dynamics over the last decade, e.g. the cited studies showing links between calving, shear margin degradation and changes in ice speed; also the very low basal stresses found far inland of the grounding line. There is a feeling that this is not replicated in other places round Antarctica, though there is actually little concrete evidence of that. For example, when carrying out inverse problems, I have not seen very low basal stresses on grounded ice in many other places, but I haven't actually done or seen proper analysis on it. I think it might be better to keep this to a short statement reflecting a generally held belief than include too much pontification. I could be persuaded otherwise though.</p>
8	<p>Lines 121-2: You refer to this past paper a few times without detail. As it relates to an important source of data in this study, a brief description of the method would be useful in this section, or at least mentioning that it uses a machine learning technique to identify crevasses.</p>	<p>I have included a short paragraph with a little more detail about this dataset.</p>
9	<p>Lines 128-49: In my opinion, these paragraphs would benefit from a little restructuring. I think the definition of $\xi = \min\{\xi_{\text{frac}}, \xi_{\text{shear}}\}$ should be introduced first, defining what the components are, before then presenting the details of how the components are calculated. This would have made it easier for me to follow, although that may be a personal preference.</p>	<p>Thank you for the good suggestion, I have changed the structure as suggested.</p>

10	<p>Lines 161-3: Could you give a reason for the choice of initial guesses? After stating that this can have a large influence on the optimisation, I feel a justification of the choice is required. Why not, for example, use a uniform guess for C or a value of 0.5 for ϕ?</p>	<p>This is a very good point! The optimisation problem will be more easily solved if the initial guess is close to the optimal solution. If we think Glen's flow law with a choice of $n = 3$ is correct, the ice is unbroken, and the temperature field we get from the thermomechanical spin-up described in the text is a good approximation, then taking $\phi = 1$ is the right choice. Even if those assumptions seem loose, $\phi = 1$ is still a natural choice as another value would require justifying why you think there is bias in the viscosity and how large you think that bias is. Regarding the choice for C, you are asking the quite a lot of the inverse solver if you supply a uniform initial guess as the field can vary by orders of magnitude. The assumption is made that under the shallow-stream approximation, most of the stress-balance on grounded ice is accounted for by sliding and gravity. In that case, a C field that accounts for the grounded ice speed will be close to the C field when the full inverse problem is performed for both control parameters over grounded and floating ice.</p> <p>I have changed the wording of this section slightly to make these points in the article.</p>
11	<p>Lines 194-7 (also Lines 226-30, 241-245): I think a summary of all experiments should be included at the end of the methods section, before going into the results. This will help to show readers exactly what you're doing in the context of methodology you've described. Introducing the exact cases during the results section seems a bit late.</p>	<p>This is a good point. I have attempted to make this clearer in the methods section by including lists of simulations for both snapshot and time-dependent problems.</p>
12	<p>Lines 203-4: The subpanel letters do not match the figure. These should be d,e,f not e,f,g</p>	<p>Thank you very much, I've fixed this now.</p>
13	<p>Lines 283-5: This is worded quite vaguely. If a reference to the previous paper is required (I would argue it is not here), be clear about what suggestion is being referred to.</p>	<p>I have changed this to read: "This suggests that observations of surface fracture on grounded ice have limited use in reducing the degeneracy associated with mixing between C and ϕ fields" and removed the reference to a previous work by the authors.</p>
14	<p>Lines 334-6: The chosen value should also be labelled on Fig.5. In fact, it would be good to have the values labelled for each circle on the figure.</p>	<p>I have added a labels to each of the circles in figure 5 as suggested.</p>

Responses to comments from Reviewer #2

Reviewer 2: This study investigates the use of surface fracture and strain rate data in constraining inversions for ice rheology. The study considers two applications – the “snapshot” inversion infers both ice viscosity and basal friction in a single timepoint and the “time-dependent” inversion infers viscosity on an ice shelf at many points in time. The study finds that the inclusion of this additional information into regularization terms can alter the estimates found by the inverse method and possibly allows for an improved physical representation of ice viscosity in the inversion. The addition of this new data appears to be most useful on floating ice.

The application of more data, particularly that of surface fracture, to constrain glaciological inversions is a potentially very useful contribution, as inverse methods are widely used to initialize models and investigate drivers of ice sheet change. The study itself is very applicable to The Cryosphere. Below I describe some comments about the work itself and the presentation.

Response: We would like to thank the reviewer for their compliments on the content of the article and insightful review.

The study focuses on the application of these new methods to a case study of Pine Island Glacier. This makes it challenging to draw a concrete conclusion about whether this new data does improve the inversion because we don’t know what the “right answer” is. Without knowing what ice softness is in Pine Island Glacier, it’s hard to know how to compare these different cases the authors present (no regularization, heuristic regularization, data-informed regularization) rather than to say that they are different in certain ways. It seems to hamper the ability for the authors to suggest that one way is “better” than the other. One way of evaluating this is comparing the misfits to see if one regularization technique improves the optimization; however, in evaluations of Figures 2-4, there doesn’t appear to be enough of a significant difference in the misfits to suggest that the data-informed regularization can produce more physical insight than the heuristic regularization. The authors are very careful and measured in the way they speak about these comparisons, which I think is a strength of this manuscript – they do acknowledge cases where the inclusion of this data does not appear to contribute to the inversion (e.g. on grounded ice). However, I still struggle with what the takeaways should be if there is such a difficulty in comparing between these cases. Possibly a clearer approach might be to test this technique on a synthetic case that approximates the PIG case study, in which a synthetic fracture field is imposed and a relationship between that fracture field and viscosity is assumed. This would provide a more straightforward way to compare between the cases presented in the manuscript and enhance the takeaways for the reader.

Response: This is a very good point, and I understand the desire to make more quantitative conclusions, however I think that attempting to do so might end up being detrimental to the study. Firstly, the ill-posedness of the problem means that we should not draw too many conclusions from the misfit. As the reviewer points out, an alternative

is to set up a problem in which the solution is essentially known a priori, e.g. synthetic examples. I did consider this when developing the work, however, I could not think of a way of doing so that would be unbiased. This would certainly have been the case had we imposed a relationship between the fracture field and viscosity in the set up of the experiments. It would also not be possible, for example, to make use of a fracture model, as there are no agreed-upon methods of doing so. Given that the effect of fractures on the rheology is always unknown prior to carrying out the inverse problem, I am still of the opinion that it is most appropriate to carry out these experiments on real data, and make-do with more qualitative statements about the success of the approach. It is my hope that there are important and interesting conclusions that people can draw from the article anyway. For example, the benefit of including fracture data in constraining damage/softness fields on floating ice is demonstrated convincingly, and the article provides a valuable demonstration that one can make use of additional data to change the solutions of the inverse problem.

Responses to specific comments from Reviewer #2

The description of the methods I found to be often hard to understand, in terms of the organization of the methods section and the wording of the explanations:

Reviewer 2		
ID	Reviewer Comment	Response
1	A bit more explanation for how fractures are identified and how those fractures are converted into a continuous field to produce f would be helpful here, especially for those that haven't read the previous papers that describe these methods.	I have added a paragraph to the methods describing briefly how crevasse data are generated. I have also added a note that the smoothing is done by convolving the maps with a Gaussian kernel.
2	Line 44: the relationship between softness and stiffness seems to imply that stiffness is bounded between 0 and 1 – is this the case, and if so, why does this need to be the case? Stiffness appears to be simply a multiplicative factors on viscosity, in which case I don't see why viscosity can't vary by orders of magnitude	(For reference, this refers to the relation $\varphi = (1-\phi)$ where φ represents softness and ϕ represents stiffness.) It is true that stiffness is bounded at the bottom by 0 (leading to an upper bound on softness of 1) which just prevents negative viscosities. In general, the stiffness is not bounded at the top by 1, meaning one can have negative softness. In our case, we do bound our stiffness at the top by 1, though it makes little difference to the solutions. It is right to say that the effective viscosities can vary by orders of magnitude, but this is almost all accounted for by Glen's flow law already. Where it is not, and we need the multiplicative scalar, important changes in viscosity are invariably on the side of reduced viscosity. We account for this with a stiffness that can reduce all the way to zero.
3	Lines 151-153 form the key description of the "snapshot" inversion and yet I found this to be challenging to understand. What is epsilon meant to represent physically? What is γ , physically? I also found it challenging to understand ξ and its relationship with ϕ . Having a clearer description of all these parameters would be very useful.	This is a good point, I have tried to make this clearer. Earlier in the manuscript, I have included the line: "In essence, $[\xi]$ should reflect our confidence in our initial guess for the ice rheology." I have then changed the line in question to read: "In the case of the snapshot inverse problem, the assumption we wish to encode in our prior for ϕ is that $\phi \sim \mathcal{N}(1, \gamma^2)$ where $\xi \rightarrow 1$, and γ is a small number related to the strength of the prior." which removes one of the parameters in the original sentence (ϵ) and states that γ is related to the strength of our prior - which goes on to be related to the regularisation parameter. Hopefully this is clearer and will be readable by most - maybe with the use of Appendix A if required.

4	The L-curve section seems to be most applicable in the methods section, as I found myself wondering while reading how the regularization parameters were chosen and whether there was an L-curve-style approach to finding them. For example, lines 165-166 mention that there is an independent search for the regularization parameters but without further information it is hard to understand what this means.	The inclusion of this section is not so much to explain the method, but to make a more general point about the use of L-curve analysis when carrying out inverse problems. Rather than moving the section, I have included a sentence in the methods section explaining that L-curve analysis is used at each juncture to tune regularisation parameters. Hopefully, that means the section on L-curves in the discussion makes slightly more sense in the context of the rest of the article.
5	The term “high” shear strain rates is used often but not defined until line 145. A definition earlier (when it is first referenced) would be useful.	I tried moving the definition further up, but it seemed a little out of place. Instead, I have included a parenthetical “defined below”. I can change this if the reviewer still thinks it is required.
6	Lines 128-130 imply that ξ is a mask of only 0 and 1 values, but Figure 1 makes it seem like ξ is continuous.	Good point. I have changed this to state that the field “goes to 0/1” rather than “is 0/1” in different areas.
7	Some of the equations (especially the regularization equations, such as Equations 10 and 11) could use much more explanation to describe what the terms mean and to remind the reader what the parameters are (I had trouble, for example, remembering the distinction between f and ξ).	I have rewritten this section, including reducing the number of parameters one needs to keep track of and introducing ξ earlier. I hope the various equations are now easier to follow.
8	The paragraph in lines 131-139 state that there are some things to note in the fracture data that are useful to understand the stress balance of PIG but the paragraph doesn’t explain what the implications to the stress balance are.	Excellent point! I have added two sentences, one about the area of grounded crevasses, and one about crevassing in the shear margins: “‘If this is indeed an area in which membrane stresses form a significant component of the stress balance, the presence of crevasses deeper than the firm layer could have implications for the dynamics of this region by changing the horizontal transmission of stress.’” and: “‘Viscous deformation in shear margins can account for a significant portion of the stress budget of an ice shelf, so changes to the large-scale rheology in such locations will influence the distribution of stress throughout the ice shelf.’”
9	Line 200 – “The phi fields in each case are substantively different...” – it took me a while to understand what the different “cases” were (it is clear upon looking at the figure but it may be helpful to state this in the text as well)	Hopefully this is clearer in the modified manuscript. The ‘cases’ are outlined in the methods section and at the beginning of the results section.
10	Line 202 – “of even slow-flowing ice streams” – I wasn’t sure what the “ice streams” were referencing here.	Good point. I have changed “ice streams” to “parts of the glacier”.

11	<p>Figures 2 and 4 – it would be helpful visually to add more labels to the colorbars rather than just the top and bottom labels. It could also be a useful diagnostic to visualize the misfit as a percentage of the observed velocity, to give some context to the absolute numbers.</p>	<p>Thank you for the comment. I have added more labels to the colourbars for all figures throughout the manuscript. Hopefully that makes things easier to interpret generally. I have not added the relative misfit as the important thing for these figures is the difference between the cases, rather than the misfits themselves. Adding an extra row to the figures makes them look a bit cluttered while not adding much.</p>
----	--	---

References

Haefeli, R.: Contribution to the Movement and the form of Ice Sheets in the Arctic and Antarctic, *Journal of Glaciology*, 3, 1133–1151, <https://doi.org/10.3189/S0022143000017548>, 1961.

Using observations of surface fracture to address ill-posed ice softness estimation over Pine Island Glacier

Trystan Surawy-Stepney¹, Stephen L. Cornford², and Anna E. Hogg¹

¹School of Earth and Environment, University of Leeds, United Kingdom

²Department of Geographical Sciences, University of Bristol, United Kingdom

Correspondence: T. Surawy-Stepney (t.surawystepney@leeds.ac.uk)

Abstract. Numerical models used to simulate the evolution of the Antarctic Ice Sheet require the specification of basal boundary conditions on stress and local deviations in the assumed material properties of the ice. In general, scalar fields ~~representing~~ relevant to these unknown components of the system are found by solving an inverse problem given observations of model state variables - typically ice flow speed. However, these optimisation problems are ~~ill-posed~~ ill posed, resulting in degenerate solutions and poor conditioning. In this study, we propose the use of fracture and strain rate data to provide prior information to the inverse problem, in an effort to better constrain the inferred ice softness compared to more heuristic regularisation techniques. We use Pine Island Glacier as a case study and consider both a ~~'snapshot'~~ snapshot inverse problem in which ice softness and basal slip parameters are sought simultaneously over the glacier as a whole, and a ~~'time-dependent'~~ time-dependent problem in which ice softness alone is sought over the floating ice shelf at regular intervals. In the first case, we construct a prior encoding the assumption that the ice softness will be close to our initial guess except from where we see fractures or high shear strain rates in satellite data. We investigate the solutions and conditioning of this data-informed inverse problem versus alternatives. ~~In the~~ The second proposed method ~~, we make~~ makes the assumption that changes to ice softness occurring on monthly-to-annual timescales ~~are will be~~ dominated by the fracturing of ice. We show that these methods can result in softness fields on floating ice that visually mimic fracture patterns without significantly affecting the ~~quality-of-the~~ solution misfit, perhaps leading to greater confidence in the softness fields as a representation of the true material properties of the ice shelf.

1 Introduction

Large-scale ice sheet models commonly treat ice within the paradigm of continuum mechanics - as a shear thinning viscous fluid; an approach that has been successful in modelling the behaviour of large ice masses relatively cheaply (e.g. Seroussi et al. (2020)). Within this framework, the flow of the ice can be accounted for in large part by a balance between gravity, viscous stress due to internal deformation and frictional stress at ice/bedrock interfaces. To close the system and allow the model to solve for ice speed, equations relating viscous and frictional stresses to ice speed are specified, informed by laboratory data and physical arguments.

The former ‘constitutive relation’ very often takes the form of Glen’s flow law:

$$25 \quad \tau_{ij} = 2\eta\dot{\epsilon}_{ij}, \quad \text{where } \eta = \frac{1}{2}A(T)^{-\frac{1}{n}}\epsilon^{\frac{1}{n}-1} \quad (1)$$

where τ_{ij} is the deviatoric stress tensor, $\dot{\epsilon}_{ij}$ is the strain rate tensor, ϵ is its second invariant, η is the strain-rate-dependent effective ice viscosity, and $A(T)$ is a temperature-dependent rate factor. The value of the exponent n is dependent on the particular mechanisms by which creep occurs within the ice and various properties of the crystal grains (e.g. Haefeli (1961)), and takes a value between 1 and $n \approx 3-4$ in most cases. (Here, we take the common reference value of $n = 3$.) It is possible

30 to treat $A(T)$ and/or n as free parameters that can be fitted to observations, given the uncertainties involved in both and the different physical mechanisms that distinguish them. ~~Here, we consider the approach in which~~ Frequently, however, these are prescribed *a priori* and a ~~‘stiffness’~~ stiffness field $\phi(x)$, ~~that scales the effective ice viscosity η ,~~ is defined over the domain to account for unknown deviations in the expected ice rheology. As such, eq. (1) becomes $\tau_{ij} = 2\phi\eta\dot{\epsilon}_{ij}$. Used in this way, ϕ approximates the effect of uncertainties in the temperature and thickness fields, regional changes in the temperature dependence

35 of Glen’s flow law, deviations from the assumed isotropy of creep deformation and, of particular interest to this study, fractures in the ice at different lengthscales. Often, a softness field φ is defined in relation to the stiffness field by $\varphi = (1 - \phi)$.

The relation between frictional stress and basal sliding speed is known as a ~~‘sliding law’~~ sliding law, and has a functional form that depends on a number of often poorly constrained factors such as the expected amount of deformation of ice around topographic features in the bed, sliding over smooth bedrock, and shearing of the sub-glacial till. A single sliding law is often

40 combined with a spatially varying ~~‘basal slip’~~ basal slip parameter $C(x)$ to approximate this stress:

$$\tau_b = Cf(\mathbf{u}). \quad (2)$$

~~Taken together~~ Given a constitutive relation and sliding law defined as above, the equations ~~considered here take the form of the shallow-stream approximation to the Cauchy momentum equations:-~~

$$\nabla \cdot [\phi h \bar{\eta} (\nabla \mathbf{u} + (\nabla \mathbf{u})^\top + 2(\nabla \cdot \mathbf{u})\mathcal{I})] - Cf(\mathbf{u}) - \rho_i g h \nabla s = 0,$$

45 where $\mathbf{u} = (u_x, u_y)^\top$ is the horizontal velocity, $\bar{\eta}$ is the vertically-integrated effective ice viscosity, ρ_i is the density of ice, h is the ice thickness and s is the ice surface. ~~In this study we use a linear sliding law $f(\mathbf{u}) = \mathbf{u}$ for ease of computing adjoint sensitivities during the inverse problem. In this article, we also refer to the “softness” field φ related to the stiffness by $\varphi = (1 - \phi)$.~~

~~In order to~~ solved by most large-scale ice sheet models contain a component dependent on ϕ (or a related scalar field performing an equivalent role) that represents viscous stress, a component dependent on C that represents frictional stress, and a component representing gravitational driving. Therefore, for an ice sheet model to simulate real ice masses accurately,

50 the fields C and ϕ are these scalar fields must be well-constrained. In practice, they are typically inferred simultaneously from observations of ice speed using inverse methods - a suite of techniques for inferring model control parameters from ob-

served state variables (MacAyeal, 1992) - (e.g. Petra et al. (2012); Arthern et al. (2015); Cornford et al. (2015); Gudmundsson et al. (2019)). ~~Unfortunately, this inverse problem is~~ Ice velocity data, rather than ice speed data, is also widely used in the community, and some methods of establishing current values for C and ϕ also incorporate rates of thickness change into the inverse problem (e.g. Larour et al. (2014); Goldberg et al. (2015)) (though this relies on the model having an automatically differentiable forward solver). We don't explicitly consider these latter kinds of 'transient' inverse problem here, though the arguments we present still apply.

60

~~Regardless of its precise implementation, this inverse problem is~~ ill-posed: the two fields (C, ϕ) are calculated from the single observed field u (the problem is "underdetermined") and the results are, resulting in solutions that are degenerate and highly dependent on noise in the input data (the problem, at least in its discrete form, is "ill-conditioned" ill-conditioned). To obtain reliable control fields, it is beneficial to replace this ill-posed problem ~~by~~ with a nearby well-posed one before solving it. The problem is sometimes simplified by solving for C only on grounded ice, and ϕ on floating ice, thereby separating the two fields spatially and removing a portion of the degeneracy that arises from the mixing of ~~C and ϕ~~ these fields (e.g. Goldberg et al. (2019)). However, though you would often expect C to be the dominant control on grounded ice speed, ~~there is little reason to be especially confident in the guess of $\phi = 1$, and getting this wrong can~~ this may well not be true everywhere and an incorrect guess for ϕ could have consequences for transient simulations. Another approach ~~, and one that shall be taken here,~~ is to regularise the solution by providing additional constraints on the control fields. Such a regularised inverse problem takes the general form of the following optimisation problem:

70

$$(C, \phi) = \operatorname{argmin}_{C, \phi} \{ \mathcal{J}_m(u, u_o) + \alpha_C \mathcal{J}_C(C) + \alpha_\phi \mathcal{J}_\phi(\phi) \}, \quad \text{s.t. } G(u, C, \phi) = 0 \quad (3)$$

where ~~$\mathcal{J}_m(u, u_o) = \|u - u_o\|_2^2$~~ $\mathcal{J}_m(u, u_o)$ is a misfit function ~~functional~~ calculating the distance of the modelled ice speed model output u from the observed ice speed data u_o (often ice speed), \mathcal{J}_C and \mathcal{J}_ϕ are regularisation functions/terms for the C and ϕ fields, with strengths controlled by the parameters α_C and α_ϕ respectively, and $G(u, C, \phi) = 0$ are the momentum balance equations ~~(5)~~ solved in the model's forward problem.

75

A popular approach, aimed at improving the conditioning of the problem by suppressing the amplification of high-frequency components of the input data, is to use Tikhonov regularisation in a form that favours either low spatial frequency or low amplitude components of the solution (e.g. Morlighem et al. (2013); Habermann et al. (2013); Brinkerhoff and Johnson (2013); Cornford et al. (2015)), e.g.:

80

$$\alpha_\phi \mathcal{J}_\phi(\phi) = \alpha_\phi \int_{\Omega} |\nabla \phi|^2 d^2 \Omega. \quad (4)$$

However, this kind of regularisation is entirely heuristic and, when it comes to distinguishing C and ϕ , relies on assumed differences in the lengthscales over which changes in the control fields can influence strain rates. Generally, in regions without

85 significant shear, these lengthscales are not easily distinguished, and degeneracies between solutions for C and ϕ proliferate. Additional difficulties arise when a control field contains distinct contributions with different spatial frequencies. For example, uncertainty in englacial temperature can vary on the scales of long-term atmospheric or geothermal heat sources, or over the width of a shear margin. Often, an imperfect but acceptable lengthscale is found by searching parameter space informed by heuristics such as L-curve analysis (Hansen and O’Leary, 1993; Hansen, 1994).

90

The aim of this study is to investigate whether the introduction of genuine prior information into the inverse problem ~~can result in substantively different solutions, and whether these solutions~~ results in solutions that are more appealing than those found using other, heuristic regularisation methods.

95 Previous studies have investigated instances in which softness fields found through solving inverse problems have mirrored observed fracture features (Borstad et al., 2013; Surawy-Stepney et al., 2023a) - suggesting that the presence of fractures has the potential to dominate ϕ . With recent advancements in observational methods for locating fractures in remote sensing data (Lai et al., 2020; Izeboud and Lhermitte, 2023; Zhao et al., 2022; Surawy-Stepney et al., 2023b), we are moving towards reliable data that can be used to inform us at least about this specific component of the softness field. Ranganathan et al. (2021)
100 showed previously that the use of strain rate data to weight the regularisation of C and ϕ has the potential to reduce mixing between these control fields. The work presented here follows quite naturally from these results.

Here, we investigate two ways in which fracture and strain-rate observations can be used to inform the inverse problem to replace or complement existing heuristic methods. The first is to use ~~fracture maps (obtained from Sentinel-1 imagery--~~
105 ~~described in Surawy-Stepney et al. (2023b))~~ maps of surface fracture along with estimates of surface strain-rates to construct a prior distribution for ϕ for use in snapshot inverse problems (single optimisations carried out for a set of geometry and speed data collected at a specific instant in time). ~~This prior simply says that we expect $\phi \approx 1$ away from regions of observed fracture, or where there are high shear strain rates (which can contribute the effects of enhanced anisotropy, shear heating and microfracturing to ϕ). In practise, this is equivalent to a form of Tikhonov regularisation using a diagonal Tikhonov matrix~~
110 ~~with entries weighted away from where we expect soft ice.~~

~~We also~~ Next, we investigate the use of timeseries of fracture maps in constraining the solutions to inverse problems carried out over multiple timesteps on floating ice. We make the assumption that softness fields should vary on long timescales except from where we see changes to the pattern of fracture. ~~The use of fracture maps as a prior in the snapshot inverse problems makes an assumption about the relative contributions of different uncertainties to ϕ . For example, we have to have a certain amount~~
115 ~~of trust in the 3D temperature field we use. A more easily justified belief is that changes to ϕ on monthly-to-annual timescales are dominated by the fracturing of ice, as other contributions to ϕ are likely to vary on significantly longer timescales. With this in mind, we initialise the inverse problem with heuristic regularisation, before imposing a regularisation that penalises the changes to ϕ except where we have seen the evolution of fractures in the observational data.~~ We show, with this method these methods, that one can generate softness fields that mimic, in certain ways, the changing fracture patterns on the Pine Island Ice

120 Shelf between 2016 and 2021, without substantially affecting the ~~misfit of the problem~~solution misfit. This may have potential uses in constraining models that aim to evolve softness fields in response to englacial stresses.

2 Methods

The simulations presented in this article were performed using the BISICLES ice sheet model (Cornford et al., 2013). This is an adaptive mesh, finite volume model which we choose here to solve discretized versions of the two-dimensional shallow-stream
125 equations~~(5)~~:

$$\nabla \cdot [\phi h \bar{\eta} (\nabla \mathbf{u} + (\nabla \mathbf{u})^\top + 2(\nabla \cdot \mathbf{u}) \mathcal{I})] - Cf(\mathbf{u}) - \rho_i g h \nabla s = 0, \quad (5)$$

where $\mathbf{u} = (u_x, u_y)^\top$ is the horizontal velocity, $\bar{\eta}$ is the vertically-integrated effective ice viscosity, ρ_i is the density of ice, h is the ice thickness and s is the ice surface. In this study we use a linear sliding law $f(\mathbf{u}) = \mathbf{u}$ for ease of computing adjoint sensitivities during the inverse problem.

130

Each inverse problem we consider in this article is of the form of eq. (3), with a misfit functional of the form $\mathcal{J}_m(u, u_o) = \|u - u_o\|_2^2$. The inverse problems differ solely in the form of the regularisation terms \mathcal{J}_ϕ . We solve each in BISICLES using a non-linear conjugate gradient method (Cornford et al., 2015).

135 Each simulation is carried out over Pine Island Glacier (PIG) in the Amundsen Sea Sector of West Antarctica with a domain encompassing the whole present-day drainage basin (Zwally et al., 2012). This region was chosen as it represents a potentially strong correspondence between fracturing and ice softness, given the abundant crevasses in the shear margins, upstream of the grounding line and the regular formation of rifts near the terminus, as well as the established dynamic impact of some of this fracturing (Joughin et al., 2021; Sun and Gudmundsson, 2023). Across the rest of Antarctica, we expect the link between
140 the dynamics of ice and the extent of fracturing to be weaker in general. We use a form of the rate factor $A(T)$ described in Cuffey and Paterson (2010), with an internal energy field generated using a 100 000 year calculation in which surface temperature, thickness and velocity are held at present day values and the combined ice temperature and moisture fraction field $E = CT + Lw$ evolves toward equilibrium. We used a geometry defined by BedMachine-v3 (Morlighem, 2022), with ~~prescribed time-evolving~~ calving front positions extracted from Sentinel-1 backscatter images. Each simulation used velocity
145 and fracture data from within a five-year period between November 2016 and November 2021. We used 200 m resolution, monthly-averaged ice velocity observations made using feature tracking applied to Sentinel-1 image pairs (Wuite et al., 2021) (<https://cryoportals.enveo.at/data/>) as the input data to the cost function and to estimate shear strain rates. ~~Crevasse data was~~

Crevasse data were generated according to the methods described in Surawy-Stepney et al. (2023b). ~~The inverse problem we consider at each stage takes the form of eq. (3) and is solved in BISICLES using a non-linear conjugate gradient method~~

150

(Cornford et al., 2015). This involves the application of deep-learning-based and other computer vision techniques to synthetic aperture radar (SAR) backscatter images from the Sentinel-1 satellite clusters, at 50 m spatial resolution. This produces maps showing the locations at which the surface expressions of crevasses and rifts are visible in the SAR data and include crevasses on floating and grounded ice. Of particular interest to this study are rifts on the Pine Island ice shelf, fractures in its shear margins, and the large field of grounded crevasses extending ~ 100 km upstream of the grounding line (Fig. 1 a). We use composite fracture maps that combine data from a month of SAR backscatter images, taking into account the differing visibility of crevasses imaged from different angles. The presence of obliquely overlapping Sentinel-1 frames is another reason for the choice of PIG as the location for this study.

2.1 Fracture data assimilation in snapshot inverse problems

The snapshot problem we consider is the joint estimation of C and ϕ over Pine Island Glacier in May 2019. We use mean velocities-2019 from mean ice speeds over the month and median composite fracture maps.

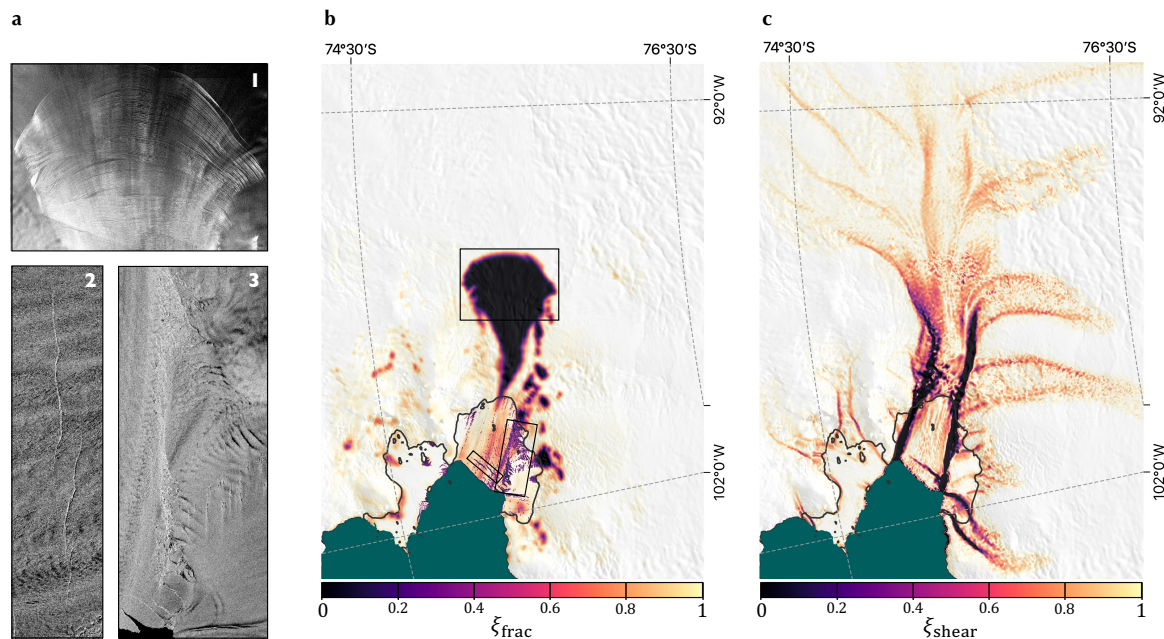


Figure 1. Contributions to the field ξ , representing, in our prior for the softness field, where we have observations of surface fracture or high shear strain rates. a) SAR backscatter images over grounded and floating parts of Pine Island Glacier from May 2019 showing regions of visible crevassing: 1) surface crevasses on the grounded ice, 2) two almost-connected rifts near the Pine Island calving front, 3) the heavily ‘damaged’ southern shear margin of Pine Island Ice Shelf. b) The component of ξ due to the observation of crevasse features, made from fracture maps developed in Surawy-Stepney et al. (2023b). Black boxes anticlockwise from the top show the locations of the SAR images a1, a2 and a3 respectively. c) The component of ξ due to the presence of high shear strain rates. Background images to b and c are the MODIS Mosaic of Antarctica (Haran et al., 2021), and grounding lines (shown in black) are according to Rignot et al. (2016).

165 ~~To construct a prior~~ The prior we construct for ϕ , ~~we~~ encodes the assumption that $\phi \approx 1$ away from regions of observed fracture or where there are high shear strain rates (which can contribute the effects of enhanced anisotropy, shear heating and microfracturing to ϕ). In practise, this is equivalent to a form of Tikhonov regularisation using a diagonal Tikhonov matrix with entries weighted away from where we expect soft ice.

170 To construct this, we first form a field ξ which ~~is~~ goes to 0 in regions which have high shear strain rates (defined below) or where fractures have been observed and ~~to~~ 1 elsewhere. ~~For the surface fracture contribution to ξ , we use monthly mosaics of fracture maps covering grounded and floating ice – slightly smoothed~~ In essence, this should reflect our confidence in our initial guess for the ice rheology. We construct it as:

$$\xi = \min\{\xi_{\text{frac}}, \xi_{\text{shear}}\} \quad (6)$$

175 where ξ_{frac} is low where we see fractures in satellite imagery (Fig. 1 b), and ξ_{shear} is low where we see high strain rates (Fig. 1 c).

180 To construct ξ_{frac} , we first smooth the fracture map for May 2019, by convolving with a Gaussian kernel, to produce contiguous fracture fields on the grounded ice. We call ~~these fracture maps f_i~~ . The fracture-map contribution to ξ is simply ~~$\xi_{\text{frac}} = 1 - f_i$~~ this fracture map f . Then $\xi_{\text{frac}} = 1 - f$ (Fig. 1 b). There are a few things to note in these fracture data of potential relevance to the stress-balance of the glacier. Firstly, we see a large contiguous area of surface fractures extending upstream from the grounding line and widening to cover a region in which previous studies have suggested membrane stresses are important in the stress-balance as basal stresses become small (Joughin et al., 2009) - ~~something we see in our own solutions for basal stress~~. SAR images of this region show uniform coverage by closely-spaced surface fractures, almost identical in appearance (Fig. 1 a1). ~~If this is indeed an area in which membrane stresses form a significant component of the stress balance, the presence of crevasses deeper than the firn layer could have implications for the dynamics of this region by changing the horizontal transmission of stress.~~ Additionally, there is a rift (really, two rifts that are almost connected) near to the ice shelf terminus that led to the calving of a large tabular iceberg in February 2020 (Fig. 1 a2) - part of a series of calving events regarded to have had significant consequences for the dynamics of Pine Island Glacier (Joughin et al., 2021). Finally, there are a large number of fractures on the southern shear margin of Pine Island Ice Shelf (Fig. 1 a3). ~~Viscous deformation in shear margins can account for a significant portion of the stress budget of an ice shelf, so changes to the large-scale rheology in such locations will influence the distribution of stress throughout the ice shelf.~~

195 We create ξ_{shear} , the strain-rate contribution to ξ , using the same velocity data that we use in our misfit ~~function~~ functional. To estimate the derivatives $\partial_i u_j$, we differentiated the velocity components using a method described in Chartrand (2017), using Tikhonov regularisation to promote smoothness (regularisation parameters were chosen with some trial-and-error, where preference was given to solutions in which regions of high shear varied smoothly over lengthscales comparable to the widths

of visible shear margins). Aligning the x -coordinate with local flow direction, we define regions of *high shear* to be those in which $|\dot{\epsilon}_{xy}| > 0.1 \text{ a}^{-1}$. This threshold is a bit discretionary, though it corresponds to stresses within the range 90 – 320 kPa of tensile strength suggested in Vaughan (1993) for a wide range of englacial temperatures. Then $\xi_{\text{shear}} = \max\{0, 1 - 10|\dot{\epsilon}_{xy}|\}$ (Fig. 1 c) and $\xi = \min\{\xi_{\text{frac}}, \xi_{\text{shear}}\}$. ~~This data picks out the shear margins of the glacier, as well as the velocity discontinuity associated with the rift close to the ice shelf calving front. (this looks like a combination of Fig. 1 b and c).~~

In the case of the snapshot inverse problem, the assumption we wish to encode ~~in our prior for ϕ is that $\phi \rightarrow 1 + \epsilon$ as is that $\phi \sim \mathcal{N}(1, \gamma^2)$ whenever $\xi \rightarrow 1$, where $\epsilon \sim \mathcal{N}(0, \gamma^2)$ and γ is a small number. Such a prior over the ϕ field related to the strength of the prior. This~~ can be written:

$$p_{\Phi}(\phi) \propto \exp\left(-\frac{1}{2\gamma^2} \int_{\Omega} (1 - \phi)^2 \xi \, d\Omega\right). \quad (7)$$

Assuming the distribution of measurement errors is isotropic, with covariance $\sigma^2 \mathcal{I}$, this translates to a regularisation term:

$$\alpha_{\phi} = \frac{\sigma^2}{\gamma^2}, \quad \mathcal{J}_{\phi}(\phi) = \int_{\Omega} (1 - \phi)^2 \xi \, d\Omega. \quad (8)$$

A greater exposition of this link between priors and regularisation parameters is given in appendix A.

~~We solve the inverse problem for the regularisation term shown in (8), as well as the heuristic regularisation (4) and no regularisation. To understand how the introduction of prior information in the form of crevasse and strain-rate data changes the solutions to the inverse problem, we compare the solutions to those found using alternative regularisation methods. Hence, for the snapshot case, we perform three inverse problems over the full domain, starting with the same initial guesses for C and ϕ , with the same regularisation on C , with the following regularisation terms for ϕ , defined in reference to eq. (3):~~

1. ~~No regularisation: $\mathcal{J}_{\phi}(\phi) = 0$.~~
2. ~~The widely-used heuristic regularisation: $\mathcal{J}_{\phi}(\phi) = \int_{\Omega} |\nabla \phi|^2 \, d\Omega$.~~
3. ~~Our data-informed regularisation: $\mathcal{J}_{\phi}(\phi) = \int_{\Omega} (1 - \phi)^2 \xi \, d\Omega$.~~

~~The results are shown in section 3.1.~~

~~The We note that the~~ initial guess for the control fields can have a large influence on the optimisation problem, ~~as the closer it is to the desired solution, the more likely the optimisation to find that solution.~~ For the ϕ field, we use an initial guess of 1 everywhere. ~~For (this is likely to be within an order of magnitude of the solution). The C field can vary by orders of magnitude, so a uniform initial guess would be a poor choice. Instead,~~ we take the view that the initial guess should be the field required to reproduce the observations on grounded ice as closely as possible with a uniform $\phi = 1$. ~~This is reflective of~~

225 an assumption that grounded ice speed is largely accounted for by balance between gravity and friction (though we know this to be untrue). Hence, before carrying out the full optimisation including both control fields, we solve an inverse problem for C with fixed $\phi = 1$, matching speeds only on grounded ice and use this as the initial guess for the joint inverse problem. This has the effect of ~~considerably~~ reducing the deviation of ϕ from 1 in the solution ~~-This and~~ has the added bonus of allowing us to search independently for the regularisation parameters α_C and α_ϕ . In general, we carry out the search for regularisation
 230 parameters using L-curve analysis (Hansen and O’Leary, 1993), though we consider this a heuristic to be used alongside other methods where necessary (section 4.3).

2.2 Fracture data assimilation through time

The use of fracture maps as a prior in the snapshot inverse problems makes an assumption about the relative contributions of
 235 different uncertainties to ϕ . For example, we have to have a certain amount of trust in the 3D temperature field we use. As previously noted, ~~the field ϕ also~~ contains contributions from sources that cannot easily be distinguished by the spatial scales on which they vary. However, it seems likely that the contribution of fracturing to ice softness ~~due to fracturing~~ varies on a shorter *temporal* scale than any other contribution. Hence, while attributing ice softness to the presence of fractures requires a large number of assumptions, we can reasonably attribute changes in ice softness ~~required by the model to fit observations~~
 240 ~~over monthly-annual over monthly-to-annual~~ timescales to the fracturing or ~~‘healing’ of ice.~~

~~Given a healing of ice, and the advection of fractures. With this in mind, we consider the case of imposing a regularisation that penalises changes to ϕ in successive timesteps, except where we have seen the evolution of fractures in the observational data. Concretely, given a~~ series of timesteps with times $\{t_i | i = 1, \dots, n\}$, separated by Δt (e.g. one month), we solve the following inverse problem for the control parameters (C_i, ϕ_i) at each timestep:

$$245 \quad (C_i, \phi_i) = \underset{C_i, \phi_i}{\operatorname{argmin}} \{ \mathcal{J}_m(u_i, u_{o_i}) + \alpha_C \mathcal{J}_C(C_i) + \frac{\alpha_\phi}{\Delta t} \mathcal{J}_\phi(\phi_i) + \frac{\alpha_t}{\Delta t} \mathcal{J}_t(\phi_i, \phi_{i-1}) \}, \quad (9)$$

~~where we have introduced the regularisation through time $\mathcal{J}_t(\phi_i, \phi_{i-1})$ relating the softness~~ This is much the same as the snapshot inverse problem defined by eq. (3), though our regularisation term $\mathcal{J}_\phi(\phi_i, \phi_{i-1})$ now includes the softness fields in the current timestep to that of the previous timestep and previous timesteps. Though not particularly sophisticated, a method such as described by Eq. (9) is immediately amenable to the introduction of fracture data ~~in the form of \mathcal{F}_t through its~~
 250 inclusion in the regularisation term \mathcal{J}_ϕ . Previous studies (Hogg et al., 2017; Selley et al., 2021) have used such a method with ~~$\mathcal{F}_t = \int_\Omega |\phi_i - \phi_{i-1}|^2 d\Omega$ $\mathcal{J}_\phi = \int_\Omega |\phi_i - \phi_{i-1}|^2 d\Omega$~~ and we modify this only slightly here. We propose the regularisation function:

$$\mathcal{J}_{t\phi} = \int_\Omega (1 - |f_i - f_{i-1}|) \times |\phi_i - \phi_{i-1}|^2 d\Omega \quad (10)$$

where f_i is the map showing the locations of fractures over the domain at time t_i . Hence, changes to the softness field are preferred in regions in which the fracture pattern has changed, with a strength that depends on the length of the timestep and the regularisation parameter α_t . ~~For these problems, we also set $\alpha_\phi = 0$.~~

We carry out such a procedure on Pine Island Glacier with 5 years of speed and fracture observations from December 2016 to December 2021, and timesteps of one month. This captures three calving events and the major disintegration of the southern shear margin of the ice shelf, and that of the calving front of Piglet Glacier (Joughin et al., 2021; Surawy-Stepney et al., 2023b). For each month, we use the mean speeds measured over that month as our observed speeds, and median fracture map composites.

We carry out two series of inverse problems, both starting with the same initial guess (ϕ field found using heuristic regularisation). One to act as a baseline, and the other reflecting our new approach:

1. Heuristic regularisation: $\mathcal{J}_\phi = \int_{\Omega} |\phi_i - \phi_{i-1}|^2 d\Omega$.
2. Data-informed regularisation: $\mathcal{J}_\phi = \int_{\Omega} (1 - |f_i - f_{i-1}|) \times |\phi_i - \phi_{i-1}|^2 d\Omega$

The results for these simulations are shown in section 3.2.

3 Results

270 3.1 Snapshot inverse problems

We begin with the results of fracture data assimilation applied to a snapshot inverse problem on Pine Island Ice Shelf ~~–We described in Sect. 2.1. As a reminder, we~~ consider how using the data-informed regularisation alters the problem compared to a case of no regularisation, and the heuristic regularisation of eq. (4). ~~We~~ As in the list shown in section 2.1, we refer to optimisations in which ϕ is unregularised as ‘case 1’, those in which we apply heuristic Tikhonov regularisation as ‘case 2’ and those in which we apply the data-informed regularisation given by eq. (8) as ‘case 3’. We look at the misfits, the output control fields and changes to the problem conditioning.

3.1.1 Softness fields

The ϕ fields in ~~each case are substantively different~~ cases 1-3 differ substantively from each other on Pine Island Glacier for this set of geometry and speed data (Fig. 2). This is true for both the grounded and floating ice. Firstly, in both cases 1 and 2 there are large deviations of ϕ from 1 far upstream of the grounding line including substantial softening in the shear margins of even slow-flowing ~~ice streams parts of the glacier~~ (Fig. 2 a, b). This is completely absent in the solution to case 3 (Fig. 2 c). Given the lower misfits in these regions (Fig. 2 ~~e, f, d, e~~) compared to case 3 (Fig. 2 ~~g, f~~), it appears that the model finds it difficult to compensate for the velocity gradients at the margins of the tributary ice streams by enhancing gradients in C where

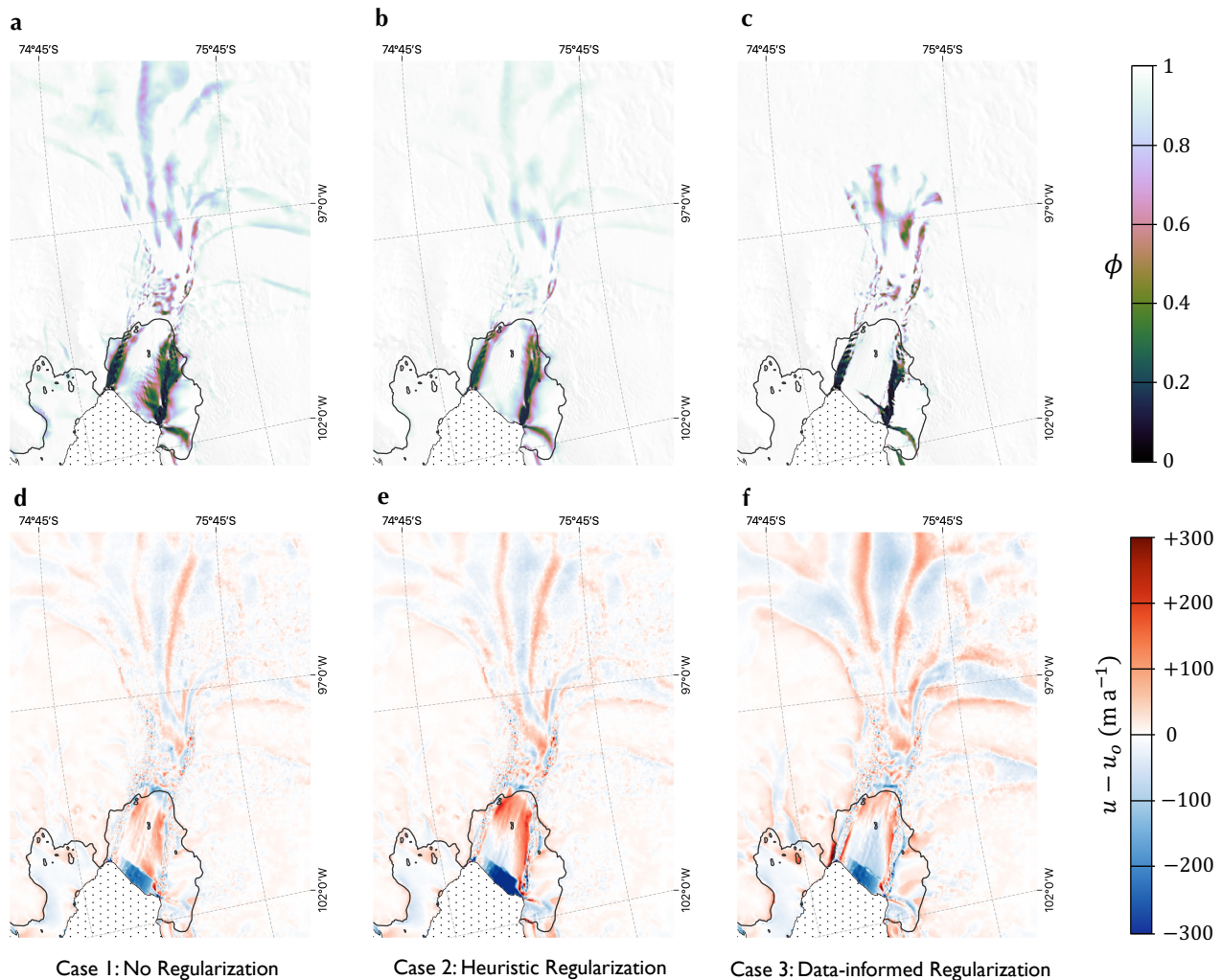


Figure 2. Solutions to the inverse problem with three methods of regularisation. a-c) Stiffness fields for the unregularised, heuristically regularised and data-informed inverse problems respectively. d-f) Misfits for the unregularised, heuristically regularised and data-informed inverse problems respectively. Background images are the MODIS Mosaic of Antarctica (Haran et al., 2021), and grounding lines (shown in black) are according to Rignot et al. (2016).

it is encouraged not to alter ϕ . In the large fractured region upstream of the grounding line (Fig. 1 a, b), the solution for case 3 shows higher amplitude deviations of ϕ from 1 than in cases 1 and 2.

The differences in ϕ between the different forms of regularisation are just as pronounced on the floating ice shelf. In cases 1 and 2, softnesses on the ice shelf are smooth and spread to large distances either side of the shear margins. In contrast, in the solution to case 3, softness is concentrated in the shear margin with larger amplitude deviations of ϕ from 1 confined to a smaller area. A portion of the solution degeneracy for ϕ on Pine Island Glacier occurs because the central shelf moves almost

entirely by pure advection. In the absence of any significant strain rates, most solutions for ϕ in this region fit the data equally well. The inclusion of an explicit prior appears to help with this by encouraging stiff ice on the central shelf.

The rift that propagated across the ice shelf at the time the speed data was collected caused a discontinuity in the data. The feature is much more clearly resolved in the solution to case 3 than case 2, and even case 1. Hence, it appears difficult for the model to assign low values of ϕ to a region very local to the rift unless encouraged to do so. This is perhaps due to the distributed influence of the ice at the terminus on the dynamics of the ice shelf as a whole (Joughin et al., 2021; Bevan et al., 2023). On the floating ice, the misfit for case 3 is considerably better than case 2 (Fig. 2 e-f).

3.1.2 The effect on problem conditioning

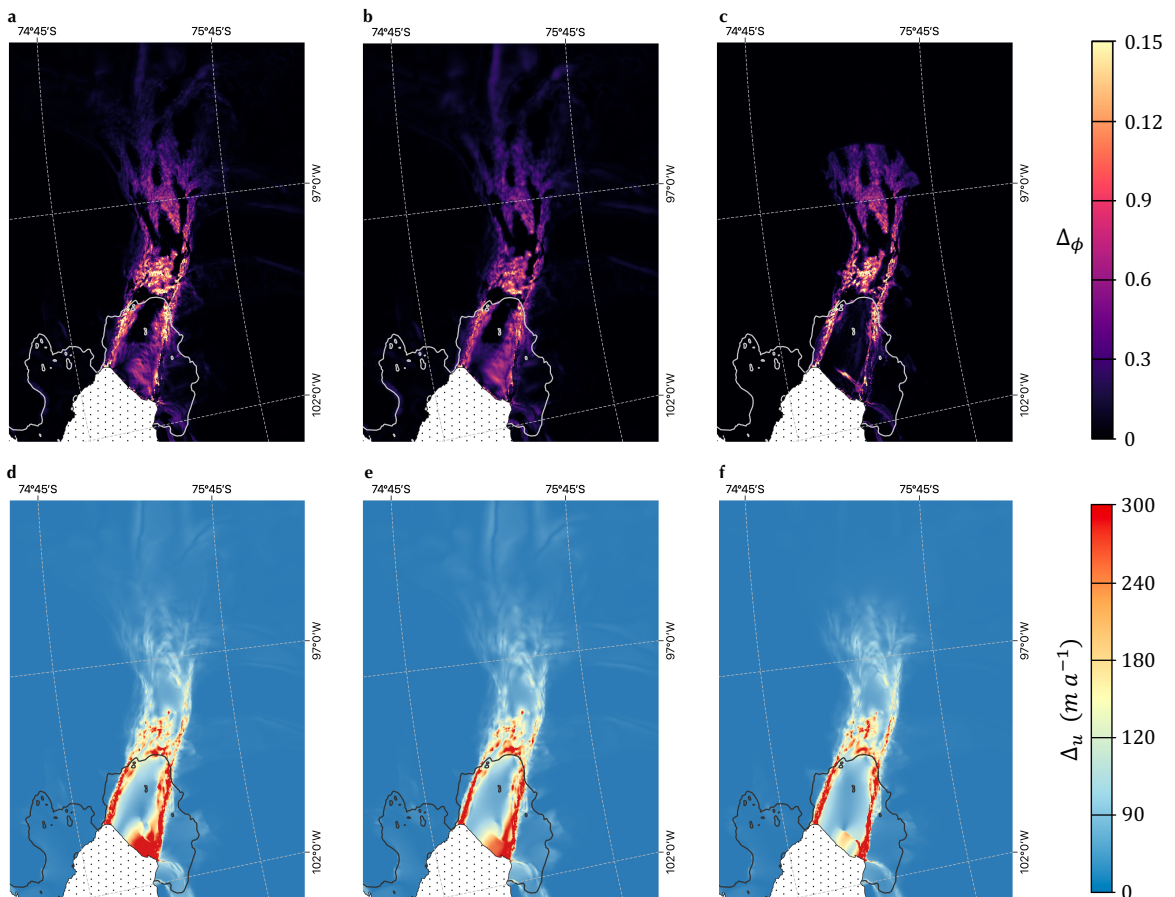


Figure 3. Variation in the solutions for the three methods of regularisation. a-c) Standard deviation in the softness fields between 10 optimisations with Gaussian noise added to the speed data for the unregularised, heuristically regularised and data-informed inverse problems respectively. d-f) Associated standard deviations in the modelled speed for the unregularised, heuristically regularised and data-informed inverse problems respectively.

300 A well conditioned problem damps the contribution of oscillatory, high frequency components of the input data, such as uncorrelated noise in the measured speed, while an ill-conditioned problem is highly sensitive to it. Bringing prior information into the inverse problem has the potential to change the conditioning by enhancing gradients in previously flat regions of the cost landscape. In order to test this change in conditioning, we investigated the impact of perturbations in the input velocity data on the spread of resulting ϕ and u fields.

305

We performed 10 inverse problems with the addition of uncorrelated Gaussian noise to the input data for the case of data-informed regularisation, heuristic regularisation and no regularisation. Noise was added with a mean of zero and standard deviation of 10% of the local speed. In each case, we measured the cell-wise standard deviation over the 10 ϕ and u output fields (Fig. 3).

310

Unsurprisingly, the regularised problems show a smaller spread in the solutions for the control fields - suggesting improved conditioning (Fig. 3 a-c). The spread of solutions for ϕ is confined in the case of the data-informed regularisation to the regions of very low ξ , while in those regions, the standard deviations are of similar magnitude to the unregularised case. This is expected because in essence, the data-informed regularisation separates regions in which high-amplitude deviations of ϕ from from 1 are penalised (where $\xi \rightarrow 1$) from regions that are entirely unregularised. The heuristic regularisation, case 2, that is explicitly devised to improve the problem conditioning indeed looks to result in the most well-conditioned problem on grounded ice. However, this is not the case on the central ice shelf, where the degeneracy described above leads to a larger solution variance than in the data-informed case. The spreads of speed (Fig. 3 d-f) reflect the spreads of the control fields.

315

3.2 Inverse problems through time

320 ~~We~~ As listed in Sec. 2.2, we consider two instances of temporal regularisation of the type described in eq. (9): the ‘data-informed’ case:

$$\mathcal{J}_{\underline{t}\phi} = \int_{\Omega} (1 - |f_i - f_{i-1}|) \times |\phi_i - \phi_{i-1}|^2 d\Omega \quad \text{and } \alpha_{\phi} = 0, \alpha_t = 5 \times 10^6, \quad (11)$$

and the ‘heuristic’ case:

$$\mathcal{J}_{\underline{t}\phi} = \int_{\Omega} |\phi_i - \phi_{i-1}|^2 d\Omega \quad \text{and } \alpha_{\phi} = 1.5 \times 10^9, \alpha_t = 10^4, \quad (12)$$

325 equivalent to that used in Selley et al. (2021).

Using fracture data in successive timesteps to weight the temporal regularisation has a significant effect on the softness fields over the five years of observations compared with the simpler approach (Fig. 4 a, b). The data-informed case leads to features of low ϕ which resemble crevasses starting to appear in the southern shear margins after ~ 18 months (black dotted arrow

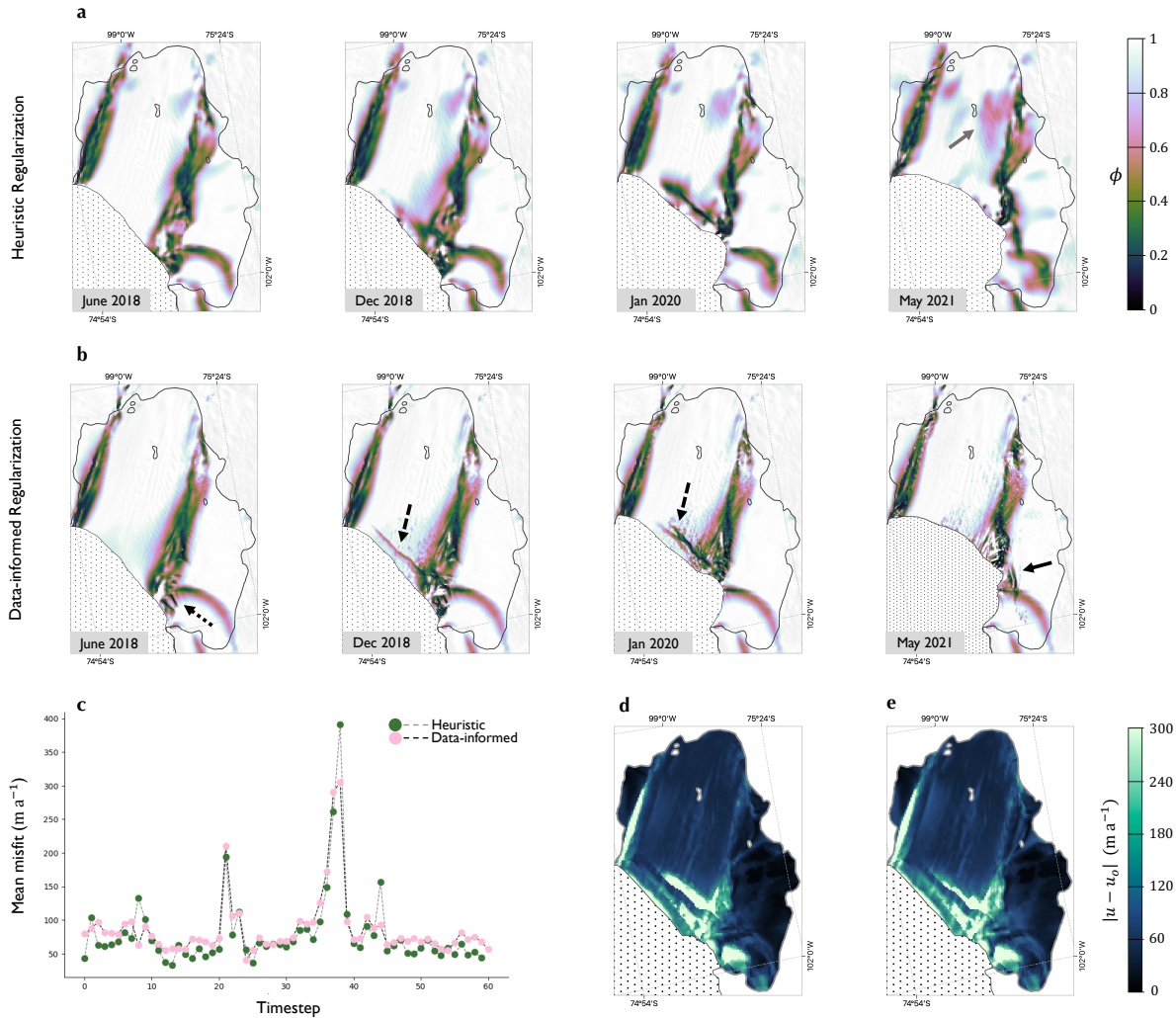


Figure 4. The evolution of the stiffness on Pine Island Ice Shelf between June 2018 and May 2021 for heuristic (a) and data-informed (b) regularisation. c) Mean misfit over the ice shelf for the two cases through time. d) Mean misfit over the ice shelf for the heuristically-regularised problem. e) Timeseries of mean misfit over the ice shelf for the data-informed and heuristically-regularised problems. Background images in a and b are the MODIS Mosaic of Antarctica (Haran et al., 2021), and grounding lines (shown in black) are according to Rignot et al. (2016).

330 Fig. 4 b). Rifts that led to the calving of large icebergs in October 2018 and February 2020 are visible as highly linear features
of soft ice in the solutions to the data-informed problem (black dashed arrows Fig. 4 b). These features are visible in Fig. 4
a, though are less easily discernible as rifts. The softness fields in the two cases appear similar by May 2021, with that of the
heuristic regularisation looking essentially like a blurred out version of the data-informed case. Both show the southerly mi-
gration of the seaward end of the southern shear margin through the time period, and, by 2021, a stripe of soft ice that connects
335 the shear margins of Pine Island and Piglet Ice Shelves. It is only clear in Fig. 4 b (black solid arrow) that this stripe of soft ice

corresponds to a number of long, parallel rifts. Diffuse blobs of softness can be seen on the central ice shelf in Fig. 4 a (May 2021, grey arrow) which are not present in the data-informed case. As the simulation contains no thickness advection and no accumulation rate is specified, it is possible that these ~~-, which are not present in the data-informed case,~~ could be the result of localised thinning. Otherwise they could once more be the result of ~~under-determinedness~~ill-posedness. This latter possibility
340 is perhaps more likely given how agnostic the model is to the values of ϕ in the central trunk and that the gravitational forcing is not modified by a change in stiffness.

Throughout the simulation period, the misfits associated with each case are very similar, with generally slightly larger mean misfits over the region in the data-informed case (Fig. 4 c, d). The exceptions to this are in the months in which calving
345 events occur - where the misfit is generally elevated as the model struggles to deal with the sudden appearance of large velocity gradients near the glacier terminus. At these times, the data-informed case does slightly better as the observations of rift growth nudge the model towards the right pattern of softening near the terminus.

4 Discussion

The problem of accurately estimating ice softness and basal slip fields from observations of ice speed is dogged by the spector
350 of ill-posedness. In an effort to improve this, we have presented two simple ways of assimilating fracture data (and in one case strain-rate data) into the inverse problem for a marine-terminating ice stream, as a way of providing the problem with **genuine** prior information. In a number of ways, the effect of these methods, their success and what we learn from the experiments ~~carried out in this study differ~~ we have carried out differs for grounded and floating ice, so we first review these separately.

4.1 Grounded ice

355 As discussed above, the presence and evolution of fractures is only a contributing factor in determining ϕ , and the efficacy of the methods ~~presented here depend~~ aimed at improving snapshot inverse problems depends on the extent to which we apportion softness to fracturing. We have seen in our example of snapshot problems over Pine Island that softness fields on grounded ice found using the data-informed regularisation vary considerably within contiguous areas of observed fracture (Fig. 2 c). If fracturing in these regions were truly the main contributor to ice softness, one would expect ϕ to be uniformly less than 1
360 this region - visually mimicking the uniform coverage of the region by surface fractures (Fig. 1 a1). This suggests that here at least, the dominant contribution to our uncertainty in the material properties of the ice softness is not the unaccounted for presence of fractures, but some combination of other factors. This is consistent with the fact that prescribing the data-informed regularisation on the grounded ice dampens the softness away from these regions of fracture but does not change the shape of the solution greatly within them. This suggests that observations of surface fracture on grounded ice have limited use in
365 reducing the degeneracy ~~between solutions caused by overlapping~~ associated with mixing between C and ϕ fields, ~~directly answering in the negative a suggestion made in Surawy-Stepney et al. (2023b).~~

In addition, this constitutes ~~a certain amount of~~ evidence that this kind of grounded surface crevasse has a limited impact on ice dynamics, despite the very low basal frictions we find in this part of Pine Island Glacier (Joughin et al., 2009) and the enhanced membrane stresses required to compensate for this. This is consistent with previous assumptions that the depths of these crevasses is only a small fraction of the ice thickness (Benn and Evans, 2014).

Finally, it is worth noting that the softness fields on grounded ice (and also substantially on floating ice) found using heuristic regularisation (Fig. 2 b) mimic many of the features of the strain rate map in Fig. 1 c. This suggests greater potential for this data to be used to constrain the softness and that the prior we are currently using doesn't fully capture our assumption that softness should be related to shear (as that of Ranganathan et al. (2021) might, for example). A better prior might, for example, be to assume softness is linear in principal strain rate. Future work should look to investigate different priors that better utilise the strain rate data at our disposal.

4.2 Floating ice

We have shown in both snapshot inverse problems and time-dependent inverse problems that the softness fields over floating ice, resulting from use of our proposed regularisation methods, appear more like what we would expect if the softening were due to fracturing/shearing compared to more heuristic regularisation methods. When encouraged to do so, the model is happy to concentrate softness in regions of observed fracture or high shear without suffering a worse misfit with the prescribed speed data. It is tempting to think that this results in softness fields that appear more likely to accurately represent the material properties of the ice shelf at the time the ice speed data was collected. Unfortunately, the ill-posedness of the problem means that methods of evaluating whether this is true do not extend far beyond a visual assessment of whether the solutions 'look right' in the context of our priors, however this is a ~~technique that should not be ignored!~~ valuable technique. Though the correlation between rheological parameters, inferred in a manner similar to that described in the heuristic regularisation case here, and crevasse data has previously been shown to be limited (Gerli et al., 2024), we have shown in both the snapshot and time-dependent cases that there are solutions to the inverse problem with at least equally good misfit in which this correlation is undoubtedly strong.

4.2.1 When would we use these methods?

The example we have chosen for the snapshot inverse problem, where a large rift can be seen on the central trunk of Pine Island Ice Shelf along with an associated discontinuity in u_o , is somewhat contrived to show the differences between the regularisation methods discussed. It is unlikely that a model-user looking to initialise a century-long simulation would choose such data, and would do better to choose data from a time more representative of a typical state of the glacier. Even if a typical state does include fractures and speed discontinuities, without a method of sensibly evolving the softness field through time, it would be reasonable to initialise a model with a smoother solution for (C, ϕ) that might be less representative of the true initial state, but ~~is~~ also less *specific* to it. Hence, softness fields found with the use of fracture data and regularisation procedures we propose

400 here are more likely to be useful in diagnostic simulations, or transient simulations with timescales on the order of years.

A major motivation for investigating these methods of constraining the inverse problem is that the time-varying solutions have potential use in evaluating models that take a continuum damage mechanics approach to parameterising the effect of fractures on large-scale ice rheology (e.g. Sun et al. (2017)). In particular, the softness fields shown in Fig. 4 b could be used to
 405 constrain the way in which a scalar damage field, that acts isotropically on the rheology, is evolved by such a model (Borstad et al., 2016).

4.3 A note on L-curves

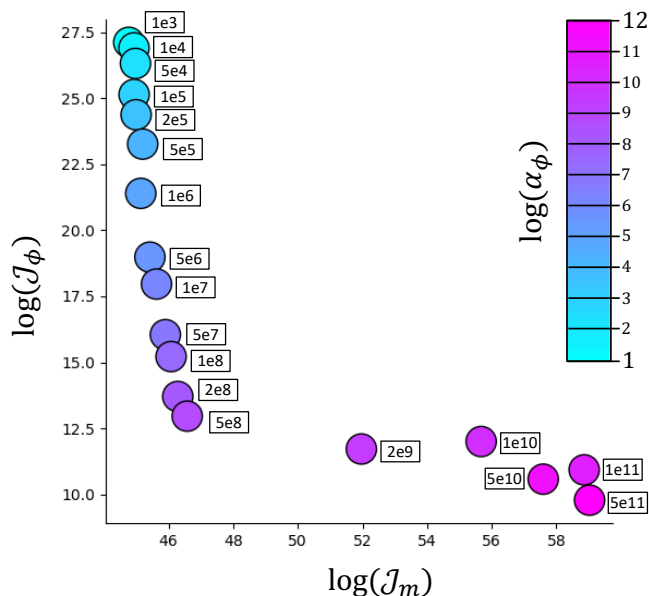


Figure 5. L-curve for the data-informed regularisation. Solution norm (y) and misfit (x) are plotted on a logarithmic scale for different choices of the regularisation parameter α_ϕ .

Fig. 5 shows, on a logarithmic scale, solution and misfit norms at convergence for a number of possible regularisation
 410 parameters α_ϕ for eq. (8), known as an L-curve (Hansen and O’Leary, 1993). Intuition suggests that one should choose the regularisation parameter at the corner of the L-curve, which balances the regularisation and misfit components of the cost function. This can be shown in some circumstances to be the point at which contributions to the solution are balanced between errors in the data and errors in the regularisation (Hansen, 2000). In our case, [for the snapshot inverse problems with data-informed regularisation](#), this is $\alpha_\phi \approx 5 \times 10^8$. However, this choice of parameter results in solutions with fewer crevasse
 415 features than we expect to see - such as the rift near the ice shelf terminus (Fig. 4 b). Hence, in practise, we choose a parameter an order of magnitude smaller, where we are satisfied with the misfit (staying on the ‘vertical branch’ of the L-curve) but can

see some of the detail we believe should be present in the softness field. Though very useful, L-curve analysis can be a blunt instrument and should always be used alongside other heuristics such as visual assessment of the control fields in deciding the regularisation parameter. Its use is based on the assertion that the preferred solution to an inverse problem is one that contains the least extraneous structure (Wolovick et al., 2023). However, for structure to be deemed ‘~~extraneous~~’extraneous, a cost function that encodes a good deal of your prior knowledge is required, which is not often available. This tendency for L-curve analysis to produce over-regularised solutions has been noted previously (e.g. Chamorro-Servent et al. (2019); Milovic et al. (2021), and notably in Recinos et al. (2023)).

5 Conclusions

425 We have introduced two ways in which fracture location data, and in one case strain rate data, can be used as prior information to inform the estimation of basal slip and ice softness fields from observations of ice speed. Applications of these methods to snapshot and time-dependent inverse problems over Pine Island Glacier show that little is gained in their use compared to the use of popular heuristic regularisation methods when considering the solutions on grounded ice. This suggests that a failure to account for the presence of fracturing does not dominate our uncertainties in the material properties of grounded ice. This is not true, however, on floating ice, where we see the resolution of fracture features in the static and time-varying softness fields without impacting the misfit, and a reduction in solution degeneracy in regions of low strain rates. This suggests that such methods can be used to provide us with softness fields that better represent the true material properties of the ice shelf at the time of the acquisition of the ice speed data. Such softness fields have potential use in diagnostic modelling, and in constraining models seeking to evolve softness fields in time.

435 *Acknowledgements.* The authors gratefully acknowledge the European Space Agency (ESA) and the European Commission for the acquisition and availability of Copernicus Sentinel-1 data. Funding is provided by ESA via the ESA Polar+ Ice Shelves project (ESA-IPL-POE-EF-cb-LE-2019-834) and the SO-ICE project (ESA AO/1-10461/20/I-NB) to AEH which both are part of the ESA Polar Science Cluster. Funding is provided from NERC via the DeCAdeS project (NE/T012757/1) and the UK EO Climate Information Service (NE/X019071/1) to AEH

440 *Code availability.* The BISICLES Ice Sheet Model is open source and the code is available at: <https://commons.lbl.gov/display/bisicles/BISICLES>. Additional code required to run the simulations in this study can be found at <https://zenodo.org/doi/10.5281/zenodo.13694744>.

Data availability. The authors have made available, for the purposes of review, data used in the modelling presented in this article at <https://zenodo.org/doi/10.5281/zenodo.13694744>. This includes geometry and speed data, as well as the priors, based on fracture and strain rate maps, used for the snapshot and ‘time-dependent’ inverse problems.

445 *Author contributions.* TSS and SLC designed the work. TSS carried out the model development and simulations and wrote the manuscript. All authors contributed to discussion.

Competing interests. The authors declare that they have no conflict of interest.

References

- Arthern, R. J., Hindmarsh, R. C. A., and Williams, C. R.: Flow speed within the Antarctic ice sheet and its controls inferred from satellite
450 observations, *Journal of Geophysical Research: Earth Surface*, 120, 1171–1188, <https://doi.org/https://doi.org/10.1002/2014JF003239>,
2015.
- Benn, D. I. and Evans, D. J.: *Glaciers & glaciation*, Routledge, 2014.
- Bevan, S., Cornford, S., Gilbert, L., Otosaka, I., Martin, D., and Surawy-Stepney, T.: Amundsen Sea Embayment ice-sheet
mass-loss predictions to 2050 calibrated using observations of velocity and elevation change, *Journal of Glaciology*, p. 1–11,
455 <https://doi.org/10.1017/jog.2023.57>, 2023.
- Borstad, C., Khazendar, A., Scheuchl, B., Morlighem, M., Larour, E., and Rignot, E.: A constitutive framework for predicting weakening and
reduced buttressing of ice shelves based on observations of the progressive deterioration of the remnant Larsen B Ice Shelf, *Geophysical
Research Letters*, 43, 2027–2035, <https://doi.org/https://doi.org/10.1002/2015GL067365>, 2016.
- Borstad, C. P., Rignot, E., Mouginot, J., and Schodlok, M. P.: Creep deformation and buttressing capacity of damaged ice shelves: theory and
460 application to Larsen C ice shelf, *The Cryosphere*, 7, 1931–1947, <https://doi.org/10.5194/tc-7-1931-2013>, 2013.
- Brinkerhoff, D. J. and Johnson, J. V.: Data assimilation and prognostic whole ice sheet modelling with the variationally derived, higher order,
open source, and fully parallel ice sheet model VarGlaS, *The Cryosphere*, 7, 1161–1184, <https://doi.org/10.5194/tc-7-1161-2013>, 2013.
- Calvetti, D. and Somersalo, E.: *Inverse problems: From regularization to Bayesian inference*, Wiley Interdisciplinary Reviews: Computational
Statistics, 10, e1427, 2018.
- 465 Chamorro-Servent, J., Dubois, R., and Coudière, Y.: Considering New Regularization Parameter-Choice Techniques for the Tikhonov Method
to Improve the Accuracy of Electrocardiographic Imaging, *Frontiers in Physiology*, 10, <https://doi.org/10.3389/fphys.2019.00273>, 2019.
- Chartrand, R.: Numerical differentiation of noisy, nonsmooth, multidimensional data, in: 2017 IEEE Global Conference on Signal and
Information Processing (GlobalSIP), pp. 244–248, <https://doi.org/10.1109/GlobalSIP.2017.8308641>, 2017.
- Cornford, S. L., Martin, D. F., Graves, D. T., Ranken, D. F., Le Brocq, A. M., Gladstone, R. M., Payne, A. J., Ng, E. G., and
470 Lipscomb, W. H.: Adaptive mesh, finite volume modeling of marine ice sheets, *Journal of Computational Physics*, 232, 529–549,
<https://doi.org/10.1016/j.jcp.2012.08.037>, 2013.
- Cornford, S. L., Martin, D. F., Payne, A. J., Ng, E. G., Le Brocq, A. M., Gladstone, R. M., Edwards, T. L., Shannon, S. R., Agosta, C., van den
Broeke, M. R., Hellmer, H. H., Krinner, G., Ligtenberg, S. R. M., Timmermann, R., and Vaughan, D. G.: Century-scale simulations of the
response of the West Antarctic Ice Sheet to a warming climate, *The Cryosphere*, 9, 1579–1600, <https://doi.org/10.5194/tc-9-1579-2015>,
475 2015.
- Cuffey, K. M. and Paterson, W. S. B.: *The physics of glaciers*, Academic Press, 2010.
- Gerli, C., Rosier, S., Gudmundsson, G. H., and Sun, S.: Weak relationship between remotely detected crevasses and inferred ice rheological
parameters on Antarctic ice shelves, *The Cryosphere*, 18, 2677–2689, <https://doi.org/10.5194/tc-18-2677-2024>, 2024.
- Goldberg, D. N., Heimbach, P., Joughin, I., and Smith, B.: Committed retreat of Smith, Pope, and Kohler Glaciers over the next 30 years
480 inferred by transient model calibration, *The Cryosphere*, 9, 2429–2446, <https://doi.org/10.5194/tc-9-2429-2015>, 2015.
- Goldberg, D. N., Gourmelen, N., Kimura, S., Millan, R., and Snow, K.: How Accurately Should We Model Ice Shelf Melt Rates?, *Geophysical
Research Letters*, 46, 189–199, <https://doi.org/https://doi.org/10.1029/2018GL080383>, 2019.
- Gudmundsson, G. H., Paolo, F. S., Adusumilli, S., and Fricker, H. A.: Instantaneous Antarctic ice sheet mass loss driven by thinning ice
shelves, *Geophysical Research Letters*, 46, 13 903–13 909, <https://doi.org/https://doi.org/10.1029/2019GL085027>, 2019.

- 485 Habermann, M., Truffer, M., and Maxwell, D.: Changing basal conditions during the speed-up of Jakobshavn Isbræ, Greenland, *The Cryosphere*, 7, 1679–1692, <https://doi.org/10.5194/tc-7-1679-2013>, 2013.
- Haefeli, R.: Contribution to the Movement and the form of Ice Sheets in the Arctic and Antarctic, *Journal of Glaciology*, 3, 1133–1151, <https://doi.org/10.3189/S0022143000017548>, 1961.
- Hansen, P.: The L-curve and its use in the numerical treatment of inverse problems, in: *InviteComputational Inverse Problems in Electrocardiology*, WIT Press, inviteComputational Inverse Problems in Electrocardiology ; Conference date: 01-01-2000, 2000.
- 490 Hansen, P. C.: Regularization tools: A Matlab package for analysis and solution of discrete ill-posed problems, *Numerical algorithms*, 6, 1–35, <https://doi.org/10.1007/BF02149761>, 1994.
- Hansen, P. C. and O’Leary, D. P.: The Use of the L-Curve in the Regularization of Discrete Ill-Posed Problems, *SIAM Journal on Scientific Computing*, 14, 1487–1503, <https://doi.org/10.1137/0914086>, 1993.
- 495 Haran, T. M., Bohlander, J., Scambos, T. A., Painter, T. H., and Fahnestock, M. A.: MODIS Mosaic of Antarctica 2003–2004 (MOA2004) Image Map, Version 2, <https://doi.org/10.5067/68TBT0CGJSOJ>, 2021.
- Hogg, A. E., Shepherd, A., Cornford, S. L., Briggs, K. H., Gourmelen, N., Graham, J. A., Joughin, I., Mouginot, J., Nagler, T., Payne, A. J., Rignot, E., and Wuite, J.: Increased ice flow in Western Palmer Land linked to ocean melting, *Geophysical Research Letters*, 44, 4159–4167, <https://doi.org/https://doi.org/10.1002/2016GL072110>, 2017.
- 500 Izeboud, M. and Lhermitte, S.: Damage detection on antarctic ice shelves using the normalised radon transform, *Remote Sensing of Environment*, 284, 113 359, <https://doi.org/10.1016/j.rse.2022.113359>, 2023.
- Joughin, I., Tulaczyk, S., Bamber, J. L., Blankenship, D., Holt, J. W., Scambos, T., and Vaughan, D. G.: Basal conditions for Pine Island and Thwaites Glaciers, West Antarctica, determined using satellite and airborne data, *Journal of Glaciology*, 55, 245–257, <https://doi.org/10.3189/002214309788608705>, 2009.
- 505 Joughin, I., Shapero, D., Smith, B., Dutrioux, P., and Barham, M.: Ice-shelf retreat drives recent Pine Island Glacier speedup, *Science Advances*, 7, eabg3080, <https://doi.org/10.1126/sciadv.abg3080>, 2021.
- Lai, C.-Y., Kingslake, J., Wearing, M. G., Chen, P.-H. C., Gentine, P., Li, H., Spergel, J. J., and van Wessem, J. M.: Vulnerability of Antarctica’s ice shelves to meltwater-driven fracture, *Nature*, 584, 574–578, <https://doi.org/10.1038/s41586-020-2627-8>, 2020.
- Larour, E., Utke, J., Csatho, B., Schenk, A., Seroussi, H., Morlighem, M., Rignot, E., Schlegel, N., and Khazendar, A.: Inferred basal friction and surface mass balance of the Northeast Greenland Ice Stream using data assimilation of ICESat (Ice Cloud and land Elevation Satellite) surface altimetry and ISSM (Ice Sheet System Model), *The Cryosphere*, 8, 2335–2351, <https://doi.org/10.5194/tc-8-2335-2014>, 2014.
- 510 MacAyeal, D. R.: The basal stress distribution of Ice Stream E, Antarctica, inferred by control methods, *Journal of Geophysical Research: Solid Earth*, 97, 595–603, 1992.
- Milovic, C., Prieto, C., Bilgic, B., Uribe, S., Acosta-Cabronero, J., Irrazaval, P., and Tejos, C.: Comparison of parameter optimization methods for quantitative susceptibility mapping, *Magnetic resonance in medicine*, 85, 480–494, <https://doi.org/10.1002/mrm.28435>, 2021.
- 515 Morlighem, M.: MEaSURES BedMachine Antarctica, Version 3, <https://doi.org/10.5067/FPSU0V1MWUB6>, 2022.
- Morlighem, M., Seroussi, H., Larour, E., and Rignot, E.: Inversion of basal friction in Antarctica using exact and incomplete adjoints of a higher-order model, *Journal of Geophysical Research: Earth Surface*, 118, 1746–1753, <https://doi.org/https://doi.org/10.1002/jgrf.20125>, 2013.
- 520 Petra, N., Zhu, H., Stadler, G., Hughes, T. J., and Ghattas, O.: An inexact Gauss-Newton method for inversion of basal sliding and rheology parameters in a nonlinear Stokes ice sheet model, *Journal of Glaciology*, 58, 889–903, <https://doi.org/10.3189/2012JoG11J182>, 2012.

- Ranganathan, M., Minchew, B., Meyer, C. R., and Gudmundsson, G. H.: A new approach to inferring basal drag and ice rheology in ice streams, with applications to West Antarctic Ice Streams, *Journal of Glaciology*, 67, 229–242, <https://doi.org/10.1017/jog.2020.95>, 2021.
- 525 Recinos, B., Goldberg, D., Maddison, J. R., and Todd, J.: A framework for time-dependent Ice Sheet Uncertainty Quantification, applied to three West Antarctic ice streams, *The Cryosphere Discussions*, 2023, 1–46, <https://doi.org/10.5194/tc-2023-27>, 2023.
- Rignot, E., Mouginot, J., and Scheuchl, B.: MEaSURES Antarctic Grounding Line from Differential Satellite Radar Interferometry, Version 2, boulder, Colorado USA. NASA National Snow and Ice Data Center Distributed Active Archive Center. doi: <https://doi.org/10.5067/IKBWW4RYHF1Q>. Accessed 15/01/2021., 2016.
- Selley, H. L., Hogg, A. E., Cornford, S., Dutrieux, P., Shepherd, A., Wuite, J., Floricioiu, D., Kusk, A., Nagler, T., Gilbert, L., Slater, T., and 530 Kim, T.-W.: Widespread increase in dynamic imbalance in the Getz region of Antarctica from 1994 to 2018, *Nature Communications*, 12, 1133, <https://doi.org/10.1038/s41467-021-21321-1>, 2021.
- Seroussi, H., Nowicki, S., Payne, A. J., Goelzer, H., Lipscomb, W. H., Abe-Ouchi, A., Agosta, C., Albrecht, T., Asay-Davis, X., Barthel, A., Calov, R., Cullather, R., Dumas, C., Galton-Fenzi, B. K., Gladstone, R., Gолledge, N. R., Gregory, J. M., Greve, R., Hattermann, T., Hoffman, M. J., Humbert, A., Huybrechts, P., Jourdain, N. C., Kleiner, T., Larour, E., Leguy, G. R., Lowry, D. P., Little, C. M., Morlighem, 535 M., Pattyn, F., Pelle, T., Price, S. F., Quiquet, A., Reese, R., Schlegel, N.-J., Shepherd, A., Simon, E., Smith, R. S., Straneo, F., Sun, S., Trusel, L. D., Van Breedam, J., van de Wal, R. S. W., Winkelmann, R., Zhao, C., Zhang, T., and Zwinger, T.: ISMIP6 Antarctica: a multi-model ensemble of the Antarctic ice sheet evolution over the 21st century, *The Cryosphere*, 14, 3033–3070, <https://doi.org/10.5194/tc-14-3033-2020>, 2020.
- Sun, S. and Gudmundsson, G. H.: The speedup of Pine Island Ice Shelf between 2017 and 2020: reevaluating the importance of ice damage, 540 *Journal of Glaciology*, p. 1–9, <https://doi.org/10.1017/jog.2023.76>, 2023.
- Sun, S., Cornford, S. L., Moore, J. C., Gladstone, R., and Zhao, L.: Ice shelf fracture parameterization in an ice sheet model, *The Cryosphere*, 11, 2543–2554, <https://doi.org/10.5194/tc-11-2543-2017>, 2017.
- Surawy-Stepney, T., Hogg, A. E., Cornford, S. L., and Davison, B. J.: Episodic dynamic change linked to damage on the thwaites glacier ice tongue, *Nature Geoscience*, <https://doi.org/10.1038/s41561-022-01097-9>, 2023a.
- 545 Surawy-Stepney, T., Hogg, A. E., Cornford, S. L., and Hogg, D. C.: Mapping Antarctic crevasses and their evolution with deep learning applied to satellite radar imagery, *The Cryosphere*, 17, 4421–4445, <https://doi.org/10.5194/tc-17-4421-2023>, 2023b.
- Vaughan, D. G.: Relating the occurrence of crevasses to surface strain rates, *Journal of Glaciology*, 39, 255–266, <https://doi.org/10.3189/S0022143000015926>, 1993.
- Wolovick, M., Humbert, A., Kleiner, T., and Rückamp, M.: Regularization and L-curves in ice sheet inverse models: a case study in the 550 Filchner–Ronne catchment, *The Cryosphere*, 17, 5027–5060, <https://doi.org/10.5194/tc-17-5027-2023>, 2023.
- Wuite, J., Hetzenecker, M., Nagler, T., and Scheiblauer, S.: ESA Antarctic Ice Sheet Climate Change Initiative (Antarctic_Ice_Sheet_cci): Antarctic Ice Sheet Monthly Velocity from 2017 to 2020, Derived from Sentinel-1, v1, <https://doi.org/10.5285/00fe090efc58446e8980992a617f632f>, 2021.
- Zhao, J., Liang, S., Li, X., Duan, Y., and Liang, L.: Detection of Surface Crevasses over Antarctic Ice Shelves Using SAR Imagery and Deep 555 Learning Method, *Remote Sensing*, 14, <https://doi.org/10.3390/rs14030487>, 2022.
- Zwally, H. J., Giovinetto, M. B., Beckley, M. A., and Saba, J. L.: Antarctic and Greenland drainage systems, *GSFC Cryospheric Sciences Laboratory*, 265, 2012.

Appendix A: Deriving a regularisation term from a prior distribution

560 Consider a version of the inverse problem in which the C field is known. Then the forward model solves $u(x) = f(\phi(x))$. We can replace this with the stochastic model:

$$U = f(\Phi) + E \quad (\text{A1})$$

where U , Φ and E are random variables representing modelled speed, the stiffness ϕ and an additive error respectively (Calvetti and Somersalo, 2018). Let the error be governed by the probability distribution p_E . Eq. (A1) then implies:

$$p_{U|\Phi}(u|\phi) = p_E(u - f(\phi)) \quad (\text{A2})$$

565 and Bayes' rule gives:

$$p_{\Phi|U}(\phi|u) \propto p_E(u - f(\phi))p_{\Phi}(\phi), \quad (\text{A3})$$

where $p_{\Phi}(\phi)$ constitutes our prior for the distribution of Φ .

We assume that as $\xi \rightarrow 1$, $\phi \rightarrow 1 + \epsilon$, where $\epsilon \sim \mathcal{N}(0, \gamma^2)$ $\phi \rightarrow \sim \mathcal{N}(1, \gamma^2)$. We can encode this as the following relation for Φ :

$$570 \quad \xi(1 - \Phi) = \gamma W \quad (\text{A4})$$

where γ controls how much we allow Φ to vary, and W is a Gaussian random field with zero mean and identity covariance. Then

$$p_{\Phi}(\phi) \propto \exp\left(-\frac{1}{2\gamma^2} \int_{\Omega} (1 - \phi)^2 \xi^2 d\Omega\right). \quad (\text{A5})$$

Assuming Gaussian error distribution with zero mean and isotropic covariance $\sigma^2 \mathcal{I}$, gives

$$p_E(u - f(\phi)) \propto \exp\left(-\frac{1}{2\sigma^2} \int_{\Omega} (u - f(\phi))^2 d\Omega\right) \quad (\text{A6})$$

575 Hence, from eq. (A3):

$$p_{\Phi|U}(\phi|u) \propto \exp\left\{-\frac{1}{2\sigma^2} \left(\int_{\Omega} (u - f(\phi))^2 d\Omega + \frac{\sigma^2}{\gamma^2} \int_{\Omega} (1 - \phi)^2 \xi d\Omega\right)\right\}, \quad (\text{A7})$$

making the assumption that $\xi^2 \approx \xi$.

A maximum a posteriori estimate for $\phi(x)$ given $u(x)$ is, therefore, the solution to:

$$\phi_{MAP} = \arg \min \left\{ \int_{\Omega} (u - f(\phi))^2 d\Omega + \frac{\sigma^2}{\gamma^2} \int_{\Omega} (1 - \phi)^2 \xi d\Omega \right\}, \quad (\text{A8})$$

580 i.e. a minimisation over our original cost function with:

$$\alpha_\phi = \frac{\sigma^2}{\gamma^2}, \quad \mathcal{J}_\phi(\phi) = \int_{\Omega} (1 - \phi)^2 \xi \, d\Omega. \quad (\text{A9})$$

A reasonable prior might be to allow ϕ to vary from 1 away from fractured areas ($\xi \rightarrow 1$) with a standard deviation of 0.1, corresponding to $\gamma^2 = 0.01$. Taking σ to be of order 100 m/y, this gives us a value of $\alpha_\phi \sim 10^6$ for the coefficient of the ϕ regularisation term in our initial cost function. Note, we have assumed in this analysis a spatially uniform estimate of uncertainty in our velocity observations. If a more reliable estimate of this uncertainty existed, it could be included as a modification to ξ .

585

Appendix B: Derivatives of \mathcal{J}_ϕ

The inverse problem is solved using a nonlinear conjugate gradient method. This requires the projection of the Jacobian $\nabla \mathcal{J}(\phi)$ along the direction of the residual $u - u_o$.

590

Let $\phi = \phi_0 e^q$ so that $\phi > 0$.

Define the stiffness part of the cost function as:

$$\mathcal{J}_\phi = \int_{\Omega} (1 - \phi)^2 \xi \, d\Omega \quad (\text{B1})$$

595 The Gâteaux differential is defined by the projection of the functional gradient onto the direction defined by a perturbation δq :

$$\langle \delta \mathcal{J}_\phi, \delta q \rangle = \lim_{\epsilon \rightarrow 0^+} \frac{\mathcal{J}_\phi(q + \epsilon \delta q) - \mathcal{J}_\phi(q)}{\epsilon}, \quad (\text{B2})$$

where the binary operator $\langle \cdot, \cdot \rangle$ is the inner product over the space of functions. In our case:

$$\langle \delta \mathcal{J}_\phi, \delta q \rangle = - \int_{\Omega} \delta q \phi (1 - \phi) \xi \, d\Omega \quad (\text{B3})$$

and we interpret $\phi(1 - \phi)\xi$ as the functional gradient. This is calculated in each iteration of the non-linear conjugate gradient method, and is used to update the value of q .

600